J. Ocean Univ. China (Oceanic and Coastal Sea Research)
https://doi.org/10.1007/s11802-023-5372-4
ISSN 1672-5182, 2023 22 (3): 777-789
http://www.ouc.edu.cn/xbywb/
E-mail:xbywb@ouc.edu.cn

Glutathione S-Transferase (GST) Identified from Giant Kelp *Macrocystis pyrifera* Increases the Copper Tolerance of *Synechococcus elongatus* PCC 7942

GU Zipeng[1)], REN Yudong[1)], LIANG Chengwei[1), *], ZHANG Xiaowen[2), 3)], GENG Yilin[1)], XU Dong[2), 3)], and YE Naihao[2), 3), *]

1) *College of Marine Science and Biological Engineering*, *Qingdao University of Science and Technology*, *Qingdao* 266042, *China*
2) *Yellow Sea Fisheries Research Institute*, *Chinese Academy of Fishery Sciences*, *Qingdao* 266071, *China*
3) *Function Laboratory for Marine Fisheries Science and Food Production Processes*, *Qingdao National Laboratory for Marine Science and Technology*, *Qingdao* 266071, *China*

(Received March 8, 2022; revised May 17, 2022; accepted August 30, 2022)

Abstract The glutathione S-transferases gene family plays an important regulatory role in growth and development, and responses to environmental change. In this study, six complete GST genes (*MpGST*1, *MpGST*2, *MpGST*3, *MpGST*4, *MpGST*5, and *MpGST*6) were cloned from the gametophytes of brown alga *Macrocystis pyrifera*. Subsequent bioinformatics analysis showed that these six genes encoded proteins with 202, 216, 288, 201, 205, and 201 aa, respectively. Moreover, *MpGST*3 differs from the other GST genes. Phylogenetic analysis suggested that MpGST3 belongs to the Ure2p type GST. Domain analysis suggested that the other GSTs from *M. pyrifera* belong to the soluble GST family and form an independent branch with the GSTs found in the other macroalgae, suggesting that a new GST type was formed during macroalgal evolution. GST genes were upregulated in *M. pyrifera* when 2.5 mg L^{-1} Cu ions were added to the medium. Six GST genes were integrated into the genome of *Synechococcus elongatus* PCC 7942, and their functions were verified by measuring light absorbance, photosynthetic pigment content, and photosynthetic parameters of the transformed strains under 0.3 mg L^{-1} Cu ion stress. The results showed much higher levels of various parameters in the transformed strains than in the wild strain. The transformed strains (with the MpGST genes) showed significantly enhanced resistance to Cu ion stress, while the wild strain almost died. The results of this study lay a theoretical foundation for further research on the Cu ion stress resistance function of GSTs in *M. pyrifera.*

Key words glutathione S-transferase genes; gene cloning; Cu ion stress; *Macrocystis pyrifera*; *Synechococcus elongatus* PCC 7942

1 Introduction

Brown algae are widely used in industry and agriculture with an important economic value (Khan *et al*., 2009; Andrew *et al*., 2018). With their wide distribution, brown seaweeds are exposed to a variety of environmental conditions and are capable of acclimating to a wide range of abiotic and biotic factors (Wiencke and Bischof, 2012; Shukla and Edwards, 2017). Most brown algae live in the intertidal and subtidal regions with different environmental factors such as salinity, temperature, and light (Hurd *et al*., 2014). A lot of researches have been conducted on the response of brown algae to abiotic stress. Giant kelp *Macrocystis pyrifera* (Laminariales) has a high biomass production because of its rapid growth rate, large size and life-history strategy (Navarrete *et al*., 2021). It forms dense stands over shallow rocky subtidal areas and underwater kelp beds (kelp forests), and determines the structure of the ecosystem (Bolton, 2010).

With the rapid development of industry and agriculture, the heavy metal content in natural water exceeds the standard, resulting in increasingly severe pollution problems. A certain concentration of heavy metals will not cause harm to marine organisms, and some of them are essential nutrients for algae growth and metabolism. But when their concentrations become too high, they can cause harm to algae, and the degrees of the impact vary with different degrees of pollution (Maxwell and Johnson, 2000; Jiang *et al*., 2003; Plekhanov and Chemeris, 2003). The toxicity of heavy metals to algae has become one of the key issues in pollution ecology (Collén *et al*., 2003). High concentrations of heavy metals can harm diatoms by inhibiting growth, destroying photosynthetic cells and mitochondria, causing oxidative damage, and modifying gene expression (Stauber and Florence, 1989; Cid *et al*., 1995; Rijstenbil and Gerringa, 2002; Herzi *et al*., 2013). Copper has a dual role in plant metabolism. It is an important component of oxidases (*e.g*., cytochrome oxidase and amino oxidases), and participates in electron transport chains, *e.g*., plastocyanin. But it is also highly to-

* Corresponding authors. E-mail: liangchw117@126.com
E-mail: yenh@ysfri.ac.cn

xic to plants (Fernandes and Henriques, 1991). This duality extends to reactive oxygen metabolism. Gill *et al*. (2011) showed that excess Cu ion inhibited plant pigment synthesis and photosynthesis.

Glutathione S-transferases (GSTs; EC 2.5.1.18) are ubiquitous in all organisms, and are multifunctional proteins encoded by a large gene family (Han *et al*., 2018). Plant GSTs are subdivided into 14 classes, based on their immunological cross-reactivities, protein sequence similarities, gene structures, substrate specificities, and conservation of specific residues. GSTs mainly detoxify xenobiotics by catalyzing the conjugation of reduced glutathione (GSH) to an extensive range of hydrophobic and electrophilic substrates (Frova, 2003). In addition to their detoxification functions, GSTs also play crucial roles in other physiological and developmental processes, including stress resistance, isomerization, secondary metabolism, signal transduction, as well as protecting against UV radiation, oxidative damage, and heavy metals (Sharma *et al*., 2004; Dixon and Edwards, 2010; Edwards *et al*., 2011). At present, there are many studies on the detoxification of heavy metals by GSTs, which show that increased GST expression is basically consistent with increases in metal tolerance, indicating that GSTs play a role in improving the metal tolerance of plants (Darko *et al*., 2004; Cançado *et al*., 2005; Dawood *et al*., 2012). For example, activation of GSTs has been reported in response to cadmium stress in *Chlamydomonas* sp. ICE-L (Ding *et al*., 2005). The relative level of GST genes increased in response to Cu ion stress and reached a maximum after three and five days in the marine alga *Ulva compressa* that were cultivated with 10 μmol L^{-1} Cu for 7 d (Contreras-Porcia *et al*., 2011).

To study the functions of proteins in macroalgae, it is important to develop a stable genetic transformation operating system. The target proteins can be expressed in such system for further analyses. The aim of this study was to clone the GST genes from *M. pyrifera* and construct them into the expression vector of S*ynechococcus elongatus* PCC 7942 and integrate them into the genome of *S. elongatus* PCC 7942 to investigate the function of GSTs in *M. pyrifera* under Cu ion stress. This study provides a theoretical basis for understanding the effect of GST genes on Cu ion stress in *M. pyrifera*.

2 Materials and Methods

2.1 *M. pyrifera* and *S. elongatus* PCC 7942 Strains and Culture Conditions

The gametophyte of *M. pyrifera* was provided from Yellow Sea Fisheries Research Institute, Chinese Academy of Fishery Sciences in Qingdao, China. All samples were rinsed with filtered seawater to remove visible epiphytic foreign matter. Then the samples were cultivated in sterile seawater at 10℃ for 24 h.

S. elongatus PCC 7942 was obtained from the GeneArt™ *Synechococcus* Protein Expression Kit (Thermo Fisher Scientific, Waltham, USA), and cultivated in Erlenmeyer flasks containing 100 mL of Blue-Green (BG11) Medium. The algae were cultured in a constant temperature incubator at 25℃ ± 2℃ under 100 μmol photons $m^{-2} s^{-1}$ for 7 days.

2.2 RNA Isolation and cDNA Synthesis

A 100 mg sample of cultured *M. pyrifera* gametophyte was blotted dry and then frozen and ground with liquid nitrogen. The total RNA was extracted using an E.Z.N.A. Plant RNA Kit (Omega, GA, USA). The RNA integrity and purity were tested using 2% agarose gel electrophoresis and a Nanodrop 2000 (Thermo Fisher Scientific, Walthma, USA).

The total RNA was reverse transcribed with an *Evo M-MLV* Plus 1st Strand cDNA Synthesis Kit (Accurate Biotechnology, Hunan, China) from an anchored oligo-dT primer, using the standard methods.

2.3 Cloning of GST cDNA from *M. pyrifera*

According to transcriptome sequence of *M. pyrifera* (Accession number CNP0001061 in China National GenBank), gene-specific primers (Table 1) were designed and made by Ruibo, China, containing enzyme cutting sites at both ends for construction of expression vector. GST genes were amplified using 2 × Pro *Taq* Master Mix (dye plus) (Accurate Biotechnology, Hunan, China). The PCR reaction conditions are as follows: 94℃ for 30 s; and then 30 cycles of 98℃ for 10 s, 62℃ for 30 s, and 72℃ for 1 min; and finally, 72℃ for 2 min. The PCR products were sequenced.

2.4 Sequencing and Phylogenetic Analysis

Gene structure analysis was carried out using the Gene Structure Display Server (GSDS) software (Hu *et al*., 2014). Genetic physical and chemical properties were analyzed using the online program ProtParam (https://web.expasy.org/protparam/). The functional sites and domains of the deduced amino acid sequences were predicted using the online NCBI program CDD (http://www.ncbi.nlm.nih.gov/Structure/cdd/wrpsb.cgi). MEGA-X was used to construct a phylogenetic tree (Kumar *et al*., 2018).

2.5 Quantification of Gene Expression Using qPCR

qPCR primers (Table 1) were designed based on the identified sequences. Tublin primers named Tub2 (Table 1) were used to amplify a fragment of the tublin as an internal reference gene. For the qPCR analysis, five shoots of *M. pyrifera* were incubated in 500 mL of 0.2 μm-filtered seawater without adding copper, or with 2.5 mg L^{-1} of $CuSO_4$ for 3, 6, 12 and 24 h. All experiments were conducted in triplicate. Then samples were rinsed with 100 mmol L^{-1} Tris-HCl-10 mmol L^{-1} EDTA, blotted dry, weighed, and frozen in liquid nitrogen. The total RNA and cDNA of the treated samples were obtained as described above.

Expression of GST genes were detected by qPCR using the Step One Plus™ Real-Time PCR System (Applied Biosystems, USA). qPCR reactions were performed using a SYBR Green Premix Pro *Taq* HS qPCR Kit II (Accurate Biotechnology, Hunan, China), and the reaction (qPCR) was conducted as follows: 95℃ for 30 s; then 40 cycles of 95℃ for 5 s and 60℃ for 30 s. Fragments amplified by qPCR were detected by fluorescence using the SYBR Green I included in the qPCR Kit. Samples were averaged, nor-

Table 1 Primer sequences used in this study

Primers name	Sequence (5'–3')	PCR objective
G1-F	CCCAAGCTTATGGCTCCCGTGTT	Gene cloning (*Hin*dIII)
G1-R	CGCGGATCCGGCCTCGAAGCGTA	Gene cloning (*Bam*HI)
G2-F	CCGGAATTCATGGCTTCCACCA	Gene cloning (*Eco*RI)
G2-R	CGGGGTACCCTTGGTGCTGAT	Gene cloning (*Kpn*I)
G3-F	CCGGAATTCATGCCGATTCGGT	Gene cloning (*Eco*RI)
G3-R	CGGGGTACCGGAGCTGTAGTTC	Gene cloning (*Kpn*I)
G4-F	CCGGAATTCATGGCCCCCGTATT	Gene cloning (*Eco*RI)
G4-R	CGGGGTACCGGCCTTGGAAGCGTA	Gene cloning (*Kpn*I)
G5-F	CCCAAGCTTATGAGCCCCAAGCTT	Gene cloning (*Hin*dIII)
G5-R	CGCGGATCCTGCCCTCGACTCCA	Gene cloning (*Bam*HI)
G6-F	CCGGAATTCATGGCTCCCGTATT	Gene cloning (*Eco*RI)
G6-R	CGGGGTACCCTAGGCCTTGGATG	Gene cloning (*Kpn*I)
MpGST1-F	GTTCATCAACATCTTCTCCA	Real-time PCR
MpGST1-R	CTTCCTAGCAACGTCCTC	Real-time PCR
MpGST2-F	CGGTGACAGCCACATGAA	Real-time PCR
MpGST2-R	CCAACCAAGTGGGAAGGA	Real-time PCR
MpGST3-F	CAGTTCGGTCACTTTACA	Real-time PCR
MpGST3-R	GGTAGCTTTTTCTCTCCA	Real-time PCR
MpGST4-F	TTCGCCACTGTCCAAACC	Real-time PCR
MpGST4-R	AAGCGTAGTACGCCTTCACC	Real-time PCR
MpGST5-F	CCCTACGAAAAAGATGGAAA	Real-time PCR
MpGST5-R	AGATGTCGCCAATGGAGA	Real-time PCR
MpGST6-F	ACGTACCCGGAAAGCCCTCT	Real-time PCR
MpGST6-R	GCCTCGTCCTTCTCTCCCAT	Real-time PCR
Tub2-F	ATCCAGGAGGTTTGGAAG	Real-time PCR
Tub2-R	ACTCGGAGACAAGGTCGT	Real-time PCR

Note: The restriction endonuclease action sites are underlined.

malized using the ΔΔCT method, and the mean value of the control was subtracted from mean treated values to determine the fold of change in the treated samples. The relative transcript levels were expressed as $2^{-\Delta\Delta CT}$ (Livak and Schmittgen, 2001). Data were averaged over three independent replications.

2.6 Heterologous Expression of the MpGST Genes in *S. elongatus* PCC 7942

To investigate the function of the *MpGSTs*, recombinant expression vector containing *MpGST*1–*MpGST*6 were constructed and transformed into *S. elongatus* PCC 7942 cells according to the manufacturer's instructions about GeneArt^{TM} *Synechococcus* Protein Expression Kit (Thermo Fisher Scientific, Walthma, USA). pSyn_6 vector was used in this study, and the process of heterologous expression of the MpGST genes in *S. elongatus* PCC 7942 is shown in Fig.1. The transformed strains containing *MpGST*1–*MpGST*6 were named MG1–MG6, respectively.

The genomic DNA of the transformed strain was extracted using an E.Z.N.A. HP Plant DNA Kit (Omega, GA, USA). Specific primers (Table 1) were added with genomic DNA as a template to amplify the target genes using 2×Pro *Taq* Master Mix (dye plus) (Accurate Biotechnology, Hunan, China). The PCR products were then sequenced for verification.

2.7 Determination of Enzyme Activity of the Transformed Strains

Stable culture for six days, the GST activity of the transformed strains was analyzed using a GST test kit (Comin, Suzhou, China). To monitor non-specific binding of the substrates, a complete assay mixture without the enzyme extract was used as a control. The GST activity was expressed per 10000 cells of sample.

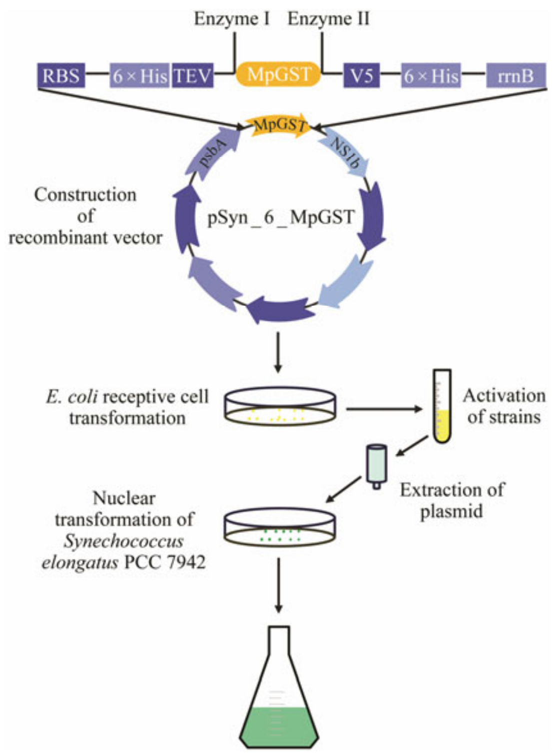

Fig.1 Process of heterologous expression of *MpGSTs* in *S. elongatus* PCC 7942.

2.8 Changes in the Physiological Indexes of the Transformed Strains Under Cu Ion Stress

The wild and transformed strains were cultured with BG11 medium to logarithmic stages, and all samples were diluted, until the OD_{750} was 0.01. A $CuSO_4{\cdot}5H_2O$ solution was added until the concentration of Cu ions in each sample was 0.3 mg L^{-1}. An equal amount of the treated algal solution was added to a multi-well plate (including a control sample without added Cu ions) and all experimental treatments were carried out in triplicate. The algae were cultured in a constant temperature incubator at 25℃±2℃ under 100 µmol photons $m^{-2}s^{-1}$. As soon as obvious growth differences were observed, the growth, pigment, and fluorescence parameters of the algae under Cu ion stress were determined to verify the function of the GST genes in *M. pyrifera*.

The algae fluid were transferred to 150 mL Erlenmeyer flasks which were sterilized for 20 min at 121℃. The previous stress treatments were repeated, then the algae were cultured in a constant temperature incubator at 25℃±2℃ under 75 µmol photons $m^{-2}s^{-1}$. The growth of algae was determined using a UV spectrophotometer to calculate the changes in algal cells at regular time intervals (2, 4, 6, 8, 10 and 12 d) during cultivation. The pigment was extracted from the algal liquid culture following the method mentioned by Xiao *et al*. (2008) and Wang *et al*. (2020) on the 6th day, and the contents of chlorophyll *a* and carotenoid were calculated following Lichtenthaler and Buschmann (2001). The maximum quantum yield of PS II (Fv/Fm) was measured using a Maxi-Imaging-PAM (Walz, Effeltrich, Germany). The treatment of algal solutions and parameter evaluation before chlorophyll *a* fluorescence measurement were performed following Zhang *et al*. (2021). The calculation of the maximum quantum yield (Fv/Fm) followed the menthod of Genty *et al*. (1989). All the experiments were conducted in triplicate.

2.9 Statistical Analysis

The Spearman rank method was used to analyze the correlation coefficients among the treatment replicates (Hauke and Kossowski, 2011). One-way analysis of variance (ANOVA) and two-way AVOVA were used to detect significance of difference in the responses between the experimental treatments and the controls. R (3.5.3) and Adobe Illustrator CS6 were used to draw and modify the graphics. Differences between mean values were considered to be significant at a probability of $P<0.05$ (Zar, 1999).

3 Results

3.1 Cloning of the GST Genes from *M. pyrifera*

Six GST cDNAs were synthesized from *M. pyrifera* using PCR. The detection results of agarose gel electrophoresis are shown in Fig.2. The results showed that the sizes of the other five gene segments were about 700 bp. *MpGST3* was about 800 bp long, roughly the same size as the target gene.

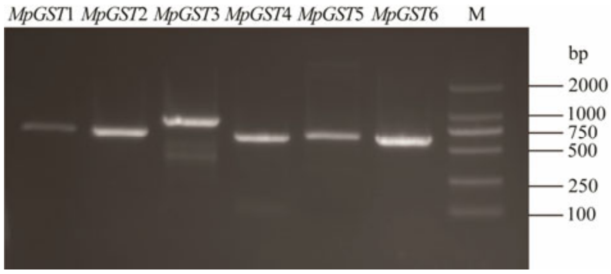

Fig.2 PCR amplification of the GST genes of *Macrocystis pyrifera*. DL2000 DNA Marker (M).

3.2 Bioinformatics Analysis of *MpGST*

Based on the cDNA sequences and the genome sequence of *M. pyrifera*, the structures of the six *MpGST*s were analyzed and showed obvious difference (Table 2, Fig.3). The basic physical and chemical properties of the proteins encoded by the GST genes of *M. pyrifera* were analyzed using the online software Prot Param. The specific results are shown in Table 3. Analysis of the PI values showed that all of the proteins were acidic, except for MpGST3. The unstable coefficients were lower than 40, except for MpGST5,

Table 2 *Macrocystis pyrifera* GST gene sequence information

Gene name	Gene length (bp)	CDS (bp)	Number of coded amino acids	Number of exons	Number of introns
MpGST1	4790	609	202	5	4
MpGST2	5420	651	216	6	5
MpGST3	8373	867	288	7	6
MpGST4	5711	606	201	5	4
MpGST5	7509	618	205	6	5
MpGST6	4449	606	201	5	4

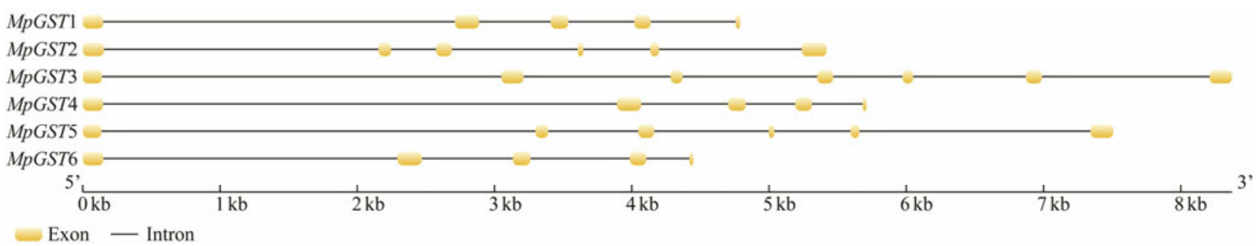

Fig.3 Structures of the *Macrocystis pyrifera* GST genes.

Table 3 Physical and chemical properties of proteins encoded by *Macrocystis pyrifera* GST genes

	MpGST1	MpGST2	MpGST3	MpGST4	MpGST5	MpGST6
Atomic composition	$C_{986}H_{1561}N_{247}O_{301}S_{12}$	$C_{1051}H_{1663}N_{268}O_{308}S_{5}$	$C_{1427}H_{2228}N_{372}O_{413}S_{13}$	$C_{980}H_{1553}N_{245}O_{293}S_{13}$	$C_{1032}H_{1636}N_{262}O_{294}S_{14}$	$C_{978}H_{1547}N_{247}O_{291}S_{12}$
Total number of atoms	3107	3296	4453	3084	3238	3075
Molecular weight	22076.44	23155.68	31620.41	21872.36	22866.76	21806.24
PI	4.71	5.34	8.2	5.14	5.45	5.46
Instability index	32.98	35.91	32.25	27.37	42.89	30.87
Grand average of hydropathicity	0.149	−0.020	−0.166	0.127	−0.011	0.085
Total number of negatively charged residues	32	27	31	26	25	26
Total number of positively charged residues	20	23	33	21	21	22

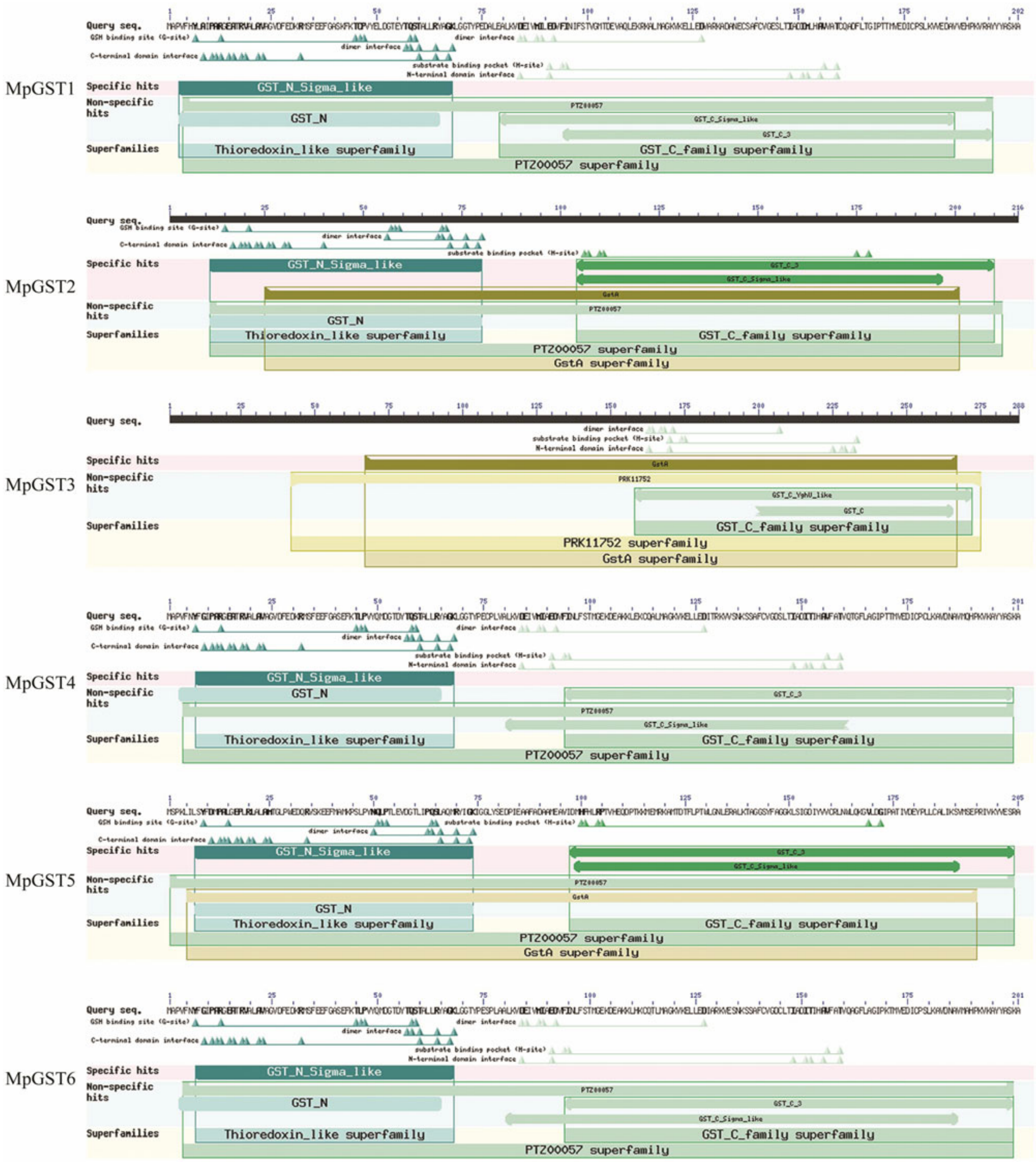

Fig.4 Functional domain analysis of *Macrocystis pyrifera* GST genes encoding proteins.

indicating that MpGST1, MpGST2, MpGST3, MpGST4 and MpGST6 were stable proteins while MpGST5 was unstable. A grand average of hydropathicity greater than zero indicates hydrophobic, and a value less than zero indicates hydrophilic. The results showed that MpGST1, MpGST4 and MpGST6 were hydrophobic proteins and MpGST2, MpGST3 and MpGST5 were hydrophilic proteins.

CDD program in NCBI website was used to analyze the conserved domain of the protein sequences encoded by the genes (Fig.4). The results showed that proteins MpGST1, MpGST2, MpGST4, MpGST5 and MpGST6 all had N-terminal domains and C-terminal domains (Fig.4). N-terminal domain indicated the Thioredoxin-like superfamily, and a C-terminal domain was unique to the GST family. The C-terminal domain belongs to the S-transferase family, and had a structure typical of soluble glutathione transferase. Therefore, it can be inferred that MpGST1, MpGST2, MpGST4, MpGST5 and MpGST6 are soluble glutathione transferases. Different from other MpGSTs, GST3 only contained conserved C-terminal domain of typical GST proteins (Fig.4).

A maximum likelihood phylogenetic tree was constructed using the complete amino acid sequences of 30 GSTs from different plant, fungal and bacterial phyla (Fig.5). The tree topology could be separated into three distinct branches or clades; angiosperms other than *Arabidopsis* and diatoms formed a separate branch, which we employed as outgroups. MpGST3 was more distant from the other MpGSTs and was located on a different branch. MpGST3 had a closer relationship to the putative GST of *Ectocarpus siliculosus*. The two MpGSTs clustered in a large clade with the GSTs of microalgae other than diatoms, *Arabidopsis*, fungi, and bacteria, and were more distantly related to the other GSTs of brown algae. The function of the putative GST has been previously confirmed and it relates to the Ure2p GST (Cock *et al*., 2012). Therefore, MpGST3 belongs to the Ure2p GST. The other GSTs of *M. pyrifera* were clustered in a branch with the GST of brown and red algae, of which MpGST2 was closely related to MpGST5, and MpGST1, MpGST4 and MpGST6 formed a separate, close-

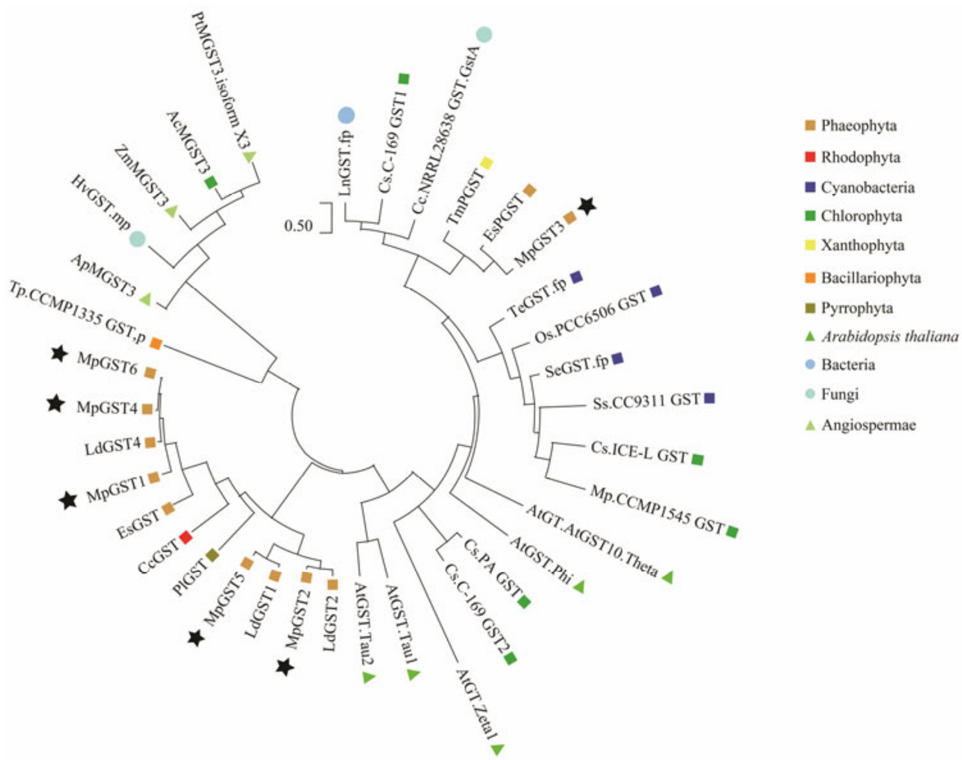

Fig.5 Phylogenetic analysis of the GST proteins. The accession numbers of each sequence are: *Leptospira noguchii* GST (WP_017215544.1), *Conidiobolus coronatus* NRRL 28638 GST (KXN73131.1), *Hesseltinella vesiculosa* GST (ORX59701.1), *Ananas comosus* GST3 (XP_020103828.1), *Populus trichocarpa* GST3 (XP_024444492.1), *Zostera marina* GST3 (KMZ69059.1), *Arabidopsis thaliana* GST.Phi (AAG30138.1), *Arabidopsis thaliana* GST.Tau1 (AAG30142.1), *Arabidopsis thaliana* GST.Tau2 (AAG30137.1), *Arabidopsis thaliana* GST10.Theta (CAA10457.1), *Arabidopsis thaliana* GST.Zeta1 (CAC19475.1), *Coccomyxa* sp. PA GST (AAC50036.1), *Coccomyxa subellipsoidea* C-169 GST1 (XP_005651120.1), *Coccomyxa subellipsoidea* C-169 GST2 (XP_005643582.1), *Chlamydomonas* sp. ICE-L GST (ADR30774.1), *Micromonas pusilla* CCMP1545 GST (XP_003060564.1), *Auxenochlorella protothecoides* GST3 (XP_011399061.1), *Thermosynechococcus elongatus* GST (WP_011056062.1), *Oscillatoria* sp. PCC 6506 GST (ZP_07108721.1), *Synechococcus* sp. CC9311 GST (WP_011619092.1), *Synechococcus elongatus* GST (WP_208677365.1), *Chondrus crispus* GST (XP_005715739.1), *Pyrocystis lunula* GST (AAN85429.1), *Thalassiosira pseudonana* CCMP1335 GST (XP_002288074.1), *Tribonema minus* GST (KAG5191659.1), *Laminaria digitata* GST4 (ABR09274.1), *Laminaria digitata* GST2 (ABR09272.1), *Laminaria digitata* GST1 (ABR09271.1), *Ectocarpus siliculosus* GST (CBJ33801.1), *Ectocarpus siliculosus* PGST (CBJ48800.1). The maximum likelihood tree was constructed using Mega-X software. A bootstrap analysis of 1000 replications were performed on the tree. Different species have been labeled accordingly. MpGSTs have all been marked with pentagons.

ly related group. MpGST1, MpGST2, MpGST4, MpGST5 and MpGST6 had higher species conservation, were more distant from the different types of GST found in *Arabidopsis thaliana*, and may form a GST type specific to large algae. Considering the information in supplementary materials in Fig.4, MpGST1, MpGST2, MpGST4, MpGST5, and MpGST6 were soluble glutathione transferases, and MpGST3 differed from them, indicating that different algal families may have evolved in different directions.

3.3 Quantitative Expression of MpGSTs Under Cu Ion Stress

qPCR was used to explore the expression patterns of the GST genes in *M. pyrifera* under Cu ion stress. Increased GST genes expression was observed following Cu ion stress treatment for 3 h, 6 h, 12 h, 24 h (Fig.6). As shown in Fig.6, the relative expression of *MpGST*3 was the highest and peaked after 12 h, while the relative expressions of *MpGST*1 and *MpGST*4 were low. Between 6 h and 12 h, the relative expression of GST genes showed an overall upward trend, but after 12 h, the expression levels began to decline and *MpGST*1 and *MpGST*4 fell below the control level (Fig.5).

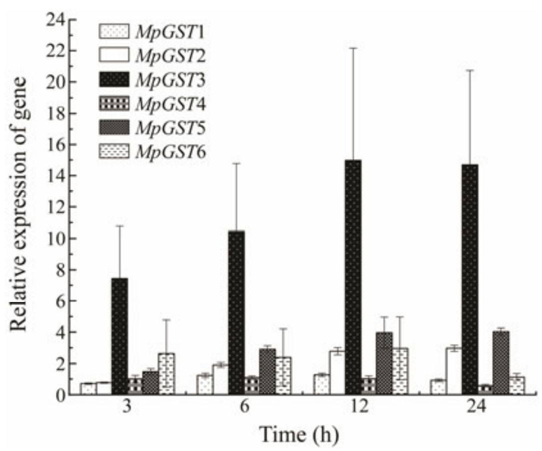

Fig.6 Relative expression of the GST genes under copper stress. The error bars indicate standard deviations (SD), $n = 3$. The same was below.

3.4 Measurement of GST Enzyme Activity in Transformed Strains

S. elongatus PCC 7942 was selected to verify gene function. The GST enzyme activities of wild and transformed strains growing to the logarithmic phase were measured simultaneously as shown in Fig.7. Except for MG6 strain, the enzyme activities of the other transformed strains were significantly different from those of the wild strains ($P < 0.05$), while MG6 showed a slight uptick ($P > 0.05$). The increased enzyme activity of the transformed strain further confirmed the success of the GST genes' heterologous expression, thus, providing a theoretical basis for the subsequent detection of physiological indicators.

3.5 Analysis of Physiological Indexes of Transformed Strains Under Cu Ion Stress

After several days of culture, all of the transformed strains

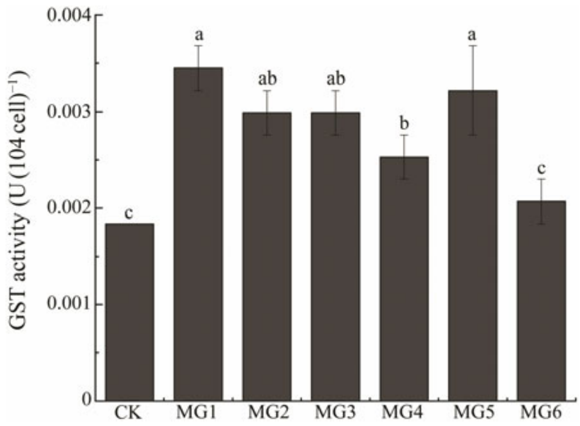

Fig.7 GST activity of genetically modified S*ynechococcus elongatus* PCC 7942. Bar of each column with different small letters mean significant difference ($P < 0.05$).

of *S. elongatus* PCC 7942 grew normally under Cu ion stress, while the wild strains could not (Fig.8). This proved the ability of the *M. pyrifera* GST genes to ameliorate the adverse effects of Cu ions to *S. elongatus* PCC 7942. To further verify the tolerance to Cu ion of the *M. pyrifera* with transformed GST genes, growth, photosynthetic pigments, photosynthetic parameters, and other physiological indicators were selected for further analyses.

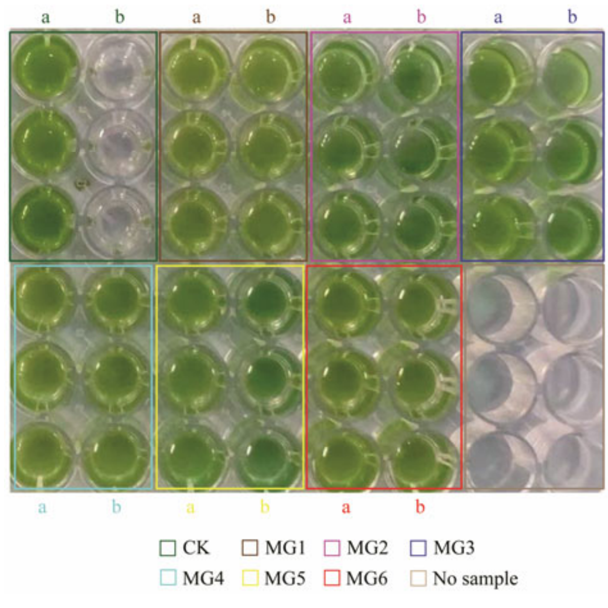

Fig.8 Preliminary multi-well plate experiment on wild-type and GSTs-transformed *Synechococcus elongatus* PCC 7942 under Cu ion stress. (a) algae cultured with general condition. (b) algae cultured with 0.3 mg L^{-1} CuSO4.

3.6 Analysis of Light Absorbance Values Under Cu Ion Stress

In this study, the light absorbance values of all of the transgenic algae except CK increased with time, and the growth rate generally increased after 6 d, while the light absorbance values of CK remained unchanged (Fig.9). MG3 strain grew best, while MG1 and MG4 grew slowly. This was consistent with the expression of the GST genes in *M. pyrifera* under Cu ion stress (Fig.9), and also with the higher enzyme activity of MG3 (Fig.7). Although MG1 had the highest enzyme activity, other physiological indicators of MG1 were not the best, which may be related to the different mechanism of action of each GST enzyme. These results indicated that Cu ions were highly toxic to wild strains, while the GST-transformed strains can resist with the toxicity and the toxicity to GST-transformed strains was not affected by exposure time.

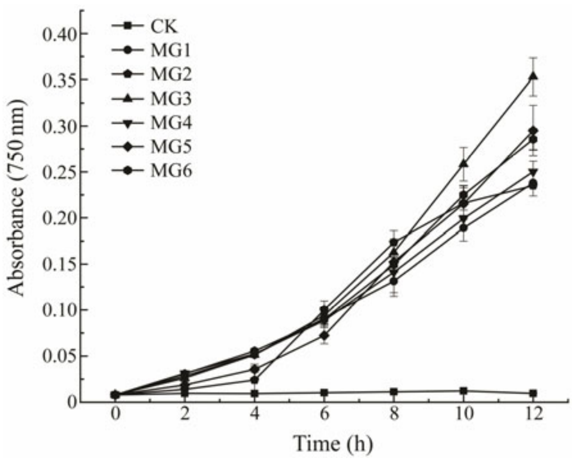

Fig.9 Growth curves of wild-type and GST-transformed *Synechococcus elongatus* PCC 7942 under copper stress.

3.7 Analysis of Pigment Content Under Cu Ion Stress

Chlorophyll is the main photosynthetic pigment. Any destruction or degradation of chlorophyll leads directly to a reduction in photosynthetic efficiency. Fig.9 shows the changes in the chlorophyll *a* (Chl*a*) content of wild and transformed strains on the 6th day with normal culture and Cu ion stress treatment. The Chl*a* content of all strains decreased after Cu ion treatment, most obviously in CK ($P<0.05$). No Chl*a* content could be detected in CK group and the wild algae were judged as dead. However, there was little difference in the Chl*a* content of MG1, MG2 and MG4 strain before and after treatment (Fig.10, $P>0.05$), which was consistent with their higher light absorbance values on the 6th day (Fig.9), and also with their higher enzyme activity (Fig.7). The Chl*a* content of MG2 in the transformed strains was the highest, but it was significantly lower than that of the wild strain. This may be because the GST-transformed strains obtained exogenous genes and affected intracellular metabolism. The specific reasons need to be verified by further experiments. All of the transformed strains had at least some Chl*a* after Cu ion treatment, which further verified the Cu ion stress resistance properties of the GST genes in *M. pyrifera*.

Carotenoids (Car) are lipid soluble and act as antioxidants and membrane stabilizers in in addition to their role in light capture (Havaux *et al*., 1998). Fig.10 shows the changes in Car content of wild and GST-transformed strains on the 6th day of normal culture and Cu ion stress treatment. As shown in Fig.10, the Car content of most strains decreased after Cu ion treatment, most obviously in CK (Fig.11, $P<0.05$), with a Car content of 0 and algae judged as dead. This was consistent with previous measurements of growth indicators (Fig.9) and Chl*a* content (Fig.10). However, the Car content of MG4 strain was slightly up-regulated under Cu ion treatment (Fig.11, $P<0.05$).

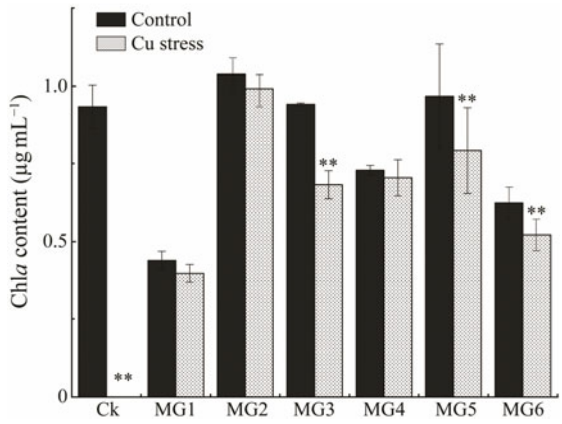

Fig.10 Chlorophyll *a* content of wild-type and GST-transformed *Synechococcus elongatus* PCC 7942 under copper stress. There was a significant difference between the two groups with asterisks ($P<0.05$).

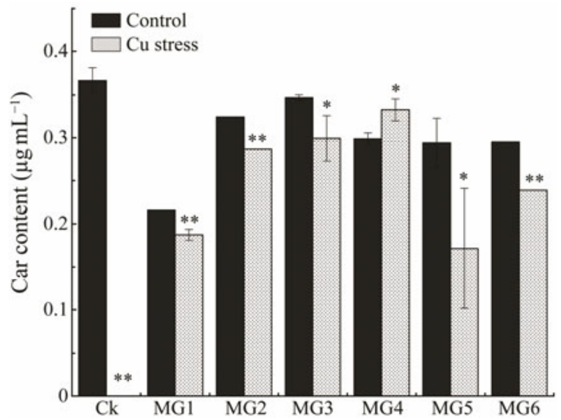

Fig.11 Carotenoid content of wild-type and GST-transformed *Synechococcus elongatus* PCC 7942 under copper stress. There was a significant difference between the two groups with asterisks ($P<0.05$).

3.8 Analysis of Photosynthetic Parameters Under Cu Ion Stress

The chlorophyll fluorescence parameter is an important index that reflects the photosynthetic activity of microalgae, and Fv/Fm represents the maximum quantum yield of PS II (Zhang *et al*., 2021). Fig.11 shows the changes in Fv/Fm of wild and GST-transformed strains on the 6th day of normal culture and Cu ion stress treatment. As shown in Fig.11, the Fv/Fm of strains decreased after Cu ion treatment, most obviously in CK group (Fig.12, $P<0.05$), with an Fv/Fm of 0 and algae were judged as dead. This was consistent with previous measurements of growth indicators (Fig.9) and pigment content (Figs.10 and 11). In addition, the Fv/Fm of MG2 strain showed the same results as the chlorophyll *a* content, with little difference before and after Cu ion stress, and better growth (Fig.11, $P>0.05$). The photosynthetic parameters were highly consistent with the photosynthetic pigment results.

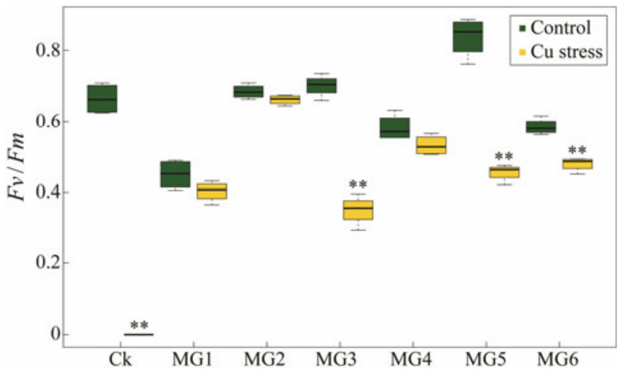

Fig.12 The maximum quantum yield (*Fv*/*Fm*) of wild-type and GST-transformed *Synechococcus elongatus* PCC 7942 under copper stress. There was a significant difference between the two groups with asterisks ($P<0.05$).

4 Discussion

Superimposed on the natural abiotic oscillations associated with the tidal cycles, seaweeds areexposed to various stresses, particularly those resulting from human industrial, urban, and agricultural activities, and their associated waste discharges (Contreras *et al*., 2010). Metal pollutants induce the production of ROS and cause an imbalance in the cellular oxidative status of cells (Rijstenbil *et al*., 1994; Okamoto *et al*., 1996). Copper is important in the reactive oxygen scavenging system, as a part of CuZn-SOD, but can also cause oxidative stress through increased production of reactive oxygen through its toxic effects on photosynthesis. Copper is a micronutrient for plants and animals, and exists naturally in coastal seawater with a concentration of $1\,\mu g\,L^{-1}$ or less (Smith *et al*., 1985; Batley, 1995; Apte and Day, 1998). It becomes toxic at higher concentrations. A protective enzyme system is formed by Glutathione S-transferases, super oxide dismutase (SOD), catalase (CAT), peroxidase (POD), *etc*., which can effectively remove reactive oxygen species and other free radicals in plants and eliminate harmful metabolites in cells, so as to protect plants from the injury caused by Cu ions. GSTs belong to a large gene family. They play an important regulatory role in growth and development, and respond to environmental changes (Wagner *et al*., 2002). Therefore, studying GSTs can help clarify the molecular mechanisms of growth and resistance to stress, and has practical significance for improving the survival of plants under stress conditions.

The types of plant GST genes include tau (U), phi (F), lambda (L), theta (T), and zeta (Z) GSTs, as well as the dehydroascorbate reductases (DHARs), tetrachlorohydroquinone dehalogenases (TCHQDs), g-subunits of the eukaryotic translation elongation factor 1B (EF1Bg), Ure2p, and microsomal prostaglandin E synthases type2 (mPGES-2). The 14 classes of GST also include recently identified classes such as hemerythrin (H), iota (I) GSTs, and glutathionyl-hydroquinone reductases (GHRs) (Lan *et al*., 2009; Liu *et al*., 2013; Yang *et al*., 2014a, 2014b; Liu *et al*., 2015; Nianiou-Obeidat *et al*., 2017). In this study, six GST genes were successfully cloned from *M. pyrifera*. In order to further study the obtained gene sequences, the physicochemical properties and domains of amino acids were analyzed and predicted using bioinformatics methods. The results showed that MpGST1, MpGST2, MpGST4, MpGST5 and MpGST6 were acidic proteins. They contain C-terminal and N-terminal domains which are unique to soluble GSTs (Perrot *et al*., 2014), which indicate that they belong to the soluble GST family. MpGST3 is a special basic protein with a larger protein size than plant GST proteins in general, and only contains a C-terminal domain. Phylogenetic analysis has shown that MpGST3 is distantly related to other MpGSTs and has confirmed that the closest putative GST from *Ectocarpus siliculosus* is the Ure2p GST. The Ure2p-type GST gene is the main GST in bacteria and funguses. Liu *et al*. (2013) speculated that the Ure2p-type GST gene may have moved from bacteria to plants. It can be inferred that *MpGST*3 is the Ure2p GST gene, based on the aggregation of fungal and bacterial GSTs on this branch. However, MpGST1, MpGST2, MpGST4, MpGST5, and MpGST6 cluster together with other brown macroalgae, and the relationship with different types of GST from *Arabidopsis* is far away, suggesting that the macroalgae themselves evolved a new type of GST.

Studies have shown that the GST gene family is involved in the response to heavy metal stress in most plants. After a treatment with $50\,\mu mol\,L^{-1}$ Cd for 7 d, the GST activity of rice roots increased significantly (Zhang *et al*., 2013). In this study, after 24 h of Cu ion treatment, the expression level of the GST genes of *M. pyrifera* increased significantly, especially *MpGST*3, after an initial downward trend at 12 h. It is possible that GST genes showing a short-lasting expression are part of the acclimation mechanism of *M. pyrifera* to buffer acute copper excess. The relative level of GST genes increased briefly in response to Cu ion stress in the marine alga *U. compressa* cultivated with $10\,\mu mol\,L^{-1}$ Cu ion (Contreras-Porcia *et al*., 2011), which is in agreement with this study.

So far, there is no precedent for successful gene transformation in *M. pyrifera*. Because *S. elongatus* PCC 7942 is easy to culture, has a small genome size, and is easily genetically manipulated by natural transformation or conjugation with *E. coli*, it is a good protein expression system for studying prokaryotic circadian rhythms, nutrient regulation, environmental responses, and lipid metabolism (Min and Golden, 2000; Atsumi *et al*., 2009; Ducat *et al*., 2011; Simkovsky *et al*., 2012; Taniguchi *et al*., 2012). In this study, *S. elongatus* 7942 was selected to verify the GST genes of *M. pyrifera.* Different concentrations of metal ions have different effects on the growth of algae. When the marine microalgae *Dunaliella tertiolecta* and *Tetraselmis suesica* were treated with different concentrations of ZnO, the algae died when ZnO concentration was higher than $81\,mg\,L^{-1}$ (Aravantinou *et al*., 2015). In this study, pre-experiments found that $0.3\,mg\,L^{-1}$ of Cu ion can kill wild *S. elongatus* PCC 7942 but allow transformed strains to grow normally. Increases in GST activity in algae are usually accompanied by differences in the growth curve under heavy metal stress. *Chlamydomonas* sp. ICE-L in the Antarctic ice was subjected to different degrees of cadmium stress, resulting in increased GST activity accompanied by a change in the growth curve (Ding *et al*., 2005). In this study, GST enzyme activity and 12-day OD_{750} were measured to test the tolerance of the GST-transformed strains to Cu ions. The results showed that the GST enzyme activities of the transformed strain were higher than those of the wild strains, which also explained why the growth of the wild strains was almost unchanged after Cu ion treatment, while the growth of the transformed strains showed an upward trend. Among them, MG3 strain showed the best growth, which corresponded to its expression level. We supposed that this was related to the difference between MpGST3 and the other MpGSTs. The growth rate of the light absorbance value generally increased after 6 d, and also formed a part of the acclimation mechanism of *M. pyrifera* to buffer acute copper excess.

Heavy metals are believed to affect the photosynthetic pigment content of algae in the following ways. Low heavy metal concentrations can promote an increase in pigment content, while high concentrations can inhibit the synthesis of chlorophyll, leading to decreased chlorophyll content and reduced photosynthetic efficiency (Brown and Newman, 2003). Chlorophyll forms the basis for photosynthesis in photo-organisms. When plants are under stress, various physiological processes are affected, directly or indirectly affecting the chlorophyll content (Li *et al*., 2008). Appropriate amounts of Cu ions contribute to the formation and stability of chlorophyll in plants, but high concentrations of Cu ions disrupt cellular metabolism and cause serious toxic effects (Zhang *et al*., 2009). Phytoplankton in the tropical freshwater Godavari River, India were subjected to Cu ion treatment. The results showed that the phytoplankton chlorophyll content increased with increasing Cu ion concentration, and then began to decrease when the concentration reached $1\times10^{-6}\,\mathrm{mol\,L^{-1}}$ (Chakraborty *et al*., 2010). In our study, the chlorophyll *a* content of transformed strains and wild strains under normal culture condition and with Cu ion stress treatment were measured on the 6th day. It was found that the Chl*a* content of the wild strain differed significantly before and after the treatment, while nearly all of the treated *S. elongatus* PCC 7942 died. The other strains grew normally, which was consistent with the growth curve. High Cu ion concentrations can inhibit cell defense function, which can destroy H_2O_2, leading to the production of free radicals and oxidative destruction of membrane lipids (Sandmann and Boger, 1980). Cu ions may react with sulphydryl groups to lower intracellular thiol concentrations, or they may interfere with electron transport. Therefore, the detrimental effects of Cu ion may cause changes in enzyme activity and kill cyanobacteria in algae (Chakraborty *et al*., 2010). Carotenoids are one of the most important light-capture pigments, and they can also be used as antioxidant and membrane stabilizer. In this study, the Car content was also determined, and the results were basically consistent with those for Chl*a*. In particular, the Car content of MG4 strain increased slightly after Cu ion stress, indicating that Car antioxidant activity increased under Cu ion stress. Collén *et al*. (2003) also found this phenomenon in a study of the changes in Car content of the red macroalga *Gracilaria tenuistipitata* under Cu ion stress.

Chlorophyll fluorescence analysis is a new technique for *in vivo* examination and diagnosis of plants. Based on photosynthetic processes, chlorophyll is used as a natural probe to study and detect the physiological status of photosynthesis in plants and the subtle effects of various external factors (Liang *et al*., 2007). Chlorophyll fluorescence parameters are closely related to photosynthesis and are true indicators of the effects of stress on plant photosynthesis (Feng, 2006). Under Cu ion stress, increasing ion concentration can significantly lead to decreasing fluorescence amplitude and increasing stress time in *Chaetocerosgracilis* spp. (Liang *et al*., 2008). When algae were subjected to Cu ion stress, Fv/Fm decreased gradually with increasing Cu ion concentration, indicating that heavy metal stress inhibited photosynthesis in algae, and that some functional PSII reaction centers became non-functional and ceased chemical activity. In this study, the Fv/Fm of transformed and wild strains before and after Cu ion stress were measured at the same time on the 6th day, and the results were completely consistent with the results of chlorophyll *a* determination. Under Cu ion stress, the wild strains showed no fluorescence, while the transformed strains showed fluorescence after treatment, further verifying the tolerance-promoting functions of GST to Cu ions in *M. pyrifera.*

However, differences in the physiological indexes of different genes before and after stress may be related to their specific mechanisms of action, and this requires further study.

5 Conclusions

In this study, we obtained six GST gene sequences from *M. pyrifera.* Bioinformatics analysis showed that the MpGST3 was more distant from other MpGSTs and might be the Ure2p type GST. Other GST from *M. pyrifera* clustered into a single branch with the GSTs from other brown macroalgae. We therefore hypothesize that brown macroalgae evolved a new GST type. Quantitative analysis showed that the expression levels of GST genes from *M. pyrifera* were up-regulated and that *MpGST*3 was at its highest under Cu ion stress. The functions of the MpGSTs were verified in *S. elongatus* PCC 7942. The results showed that MpGSTs increased the tolerance of *S. elongatus* PCC 7942 to Cu ion stress. Our study furthers our knowledge of the functions of the GSTs in *M. pyrifera*, and it laid a theoretical foundation for the cultivation of algal tolerant strains under copper pollution in the future.

Data Availability Statement

The raw data generated in this study were deposited in Genbank with accession numbers OL362284, OL362285, OL362286, OL362287, OL362288, OL362289.

Acknowledgements

This study is supported by the National Key R&D Program of China (No. 2018YFD0900305), the National Natural Science Foundation of China (No. 31770393), the Major Scientific and Technological Innovation Project of Shandong Provincial Key Research and Development Program (No. 2019JZZY020706), the Central Public-Interest Scientific Institute Basal Research Fund, CAFS (Nos. 2020TD 19 and 2020TD27), the China Agriculture Research System (CARS-50), the Taishan Scholars Funding of Shandong Province, and the Taishan Scholars Funding and Talent Projects of Distinguished Scientific Scholars in Agriculture and Young Taishan Scholars Program to DONG Xu.

Abbreviations

GSH, glutathione;
GST, glutathione S-transferase;
ROS, reactive oxygen species;
PCR, polymerase chain reaction;
qPCR, real-time quantitative polymerase chain reaction;
OD_{750}, optical density at 750 nm;
Chl*a*, chlorophyll *a*;
Car, carotenoid;
CDS, coding protein sequence;
PI, isoelectric point;
PSII, photosystem II;
CK, control.

References

Andrew, R., Reed, D. C., Harrer, S. L., and Clint, N. J., 2018. Improved estimates of net primary production, growth and standing crop of *Macrocystis pyrifera* in Southern California. *Ecology*, **99** (9): 2132, DOI: 10.1002/ecy.2440.

Apte, S. C., and Day, G. M., 1998. Dissolved metal concentrations in the Torres Strait and Gulf of Papua. *Marine Pollution Bulletin*, **36** (4): 298-304, DOI: 10.1016/S0025-326X(98)00188-X.

Aravantinou, A. F., Tsarpali, V., Dailianis, S., and Manariotis, I. D., 2015. Effect of cultivation media on the toxicity of ZnO nanoparticles to freshwater and marine microalgae. *Ecotoxicology and Environmental Safety*, **114**: 109-116, DOI: 10.1016/j.ecoenv.2015.01.016.

Atsumi, S., Higashide, W., and Liao, J. C., 2009. Direct photosynthetic recycling of carbon dioxide to isobutyraldehyde. *Nature Biotechnology*, **27** (12): 1177-1180, DOI: 10.1038/nbt.1586.

Batley, G. E., 1995. Heavy metals and tributyltin in Australian coastal and estuarine waters. In: *Pollution State of the Marine Environment Report for Australia*. Zann, L. P., and Sutton, D., eds., Great Barrier Reef Marine Park Authority, Canberra, 63-72.

Bolton, J. J., 2010. The biogeography of kelps (Laminariales, Phaeophyceae): A global analysis with new insights from recent advances in molecular phylogenetics. *Helgoland Marine Research*, **64** (4): 263-279, DOI: 10.1007/s10152-010-0211-6.

Brown, M. T., and Newman, J. E., 2003. Physiological responses of *Gracilariopsis longissima* (S.G. Gmelin) Steentoft, L.M. Iryine and Farnham (Rhodophyceae) to sublethal copper. *Aquatic Toxicology*, **64** (2): 201-213, DOI: 10.1016/S0166-445X(03)00054-7.

Cançado, G. M. A., De Rosa Jr., V. E., Fernandez, J. H., Maron, L. G., Jorge, R. A., and Menossi, M., 2005. Glutathione S-transferase and aluminum toxicity in maize. *Functional Plant Biology*, **32** (11): 1045-1055, DOI: 10.1071/FP05158.

Chakraborty, P., Babu, P., Acharyya, T., and Bandyopadhyay, D., 2010. Stress and toxicity of biologically important transition metals (Co, Ni, Cu and Zn) on phytoplankton in a tropical freshwater system: An investigation with pigment analysis by HPLC. *Chemosphere*, **80** (5): 548-553, DOI: 10.1016/j.chemosphere.2010.04.039.

Cid, A., Herrero, C., Torres, E., and Abalde, J., 1995. Copper toxicity on the marine microalga *Phaeodactylum tricornutum*: Effects on photosynthesis and related parameters. *Aquatic Toxicology*, **31** (2): 165-174, DOI: 10.1016/0166-445X(94)00071-W.

Cock, J. M., Sterck, L., Rouzé, P., Scornet, D., Allen, A. E., Amoutzias, G., *et al*., 2012. The *Ectocarpus* genome and the independent evolution of multicellularity in brown algae. *Nature*, **465** (7298): 617-621, DOI: 10.1038/nature09016.

Collén, J., Pioto, E., Pedersén, M., and Colepicolo, P., 2003. Induction of oxidative stress in the redmacroalga *Gracilaria tenuistipitata* by pollutant metals. *Archives of Environmental Contamination and Toxicology*, **45** (3): 337-342, DOI: 10.1007/s00244-003-0196-0.

Contreras, L., Moenne, A., and Correa, J. A., 2010. Antioxidant responses in *Scytosiphon lomentaria* (Phaeophyceae) inhabiting copper-enriched coastal environments. *Journal of Phycology*, **41** (6): 1184-1195, DOI: 10.1111/j.1529-8817.2005.00151.x.

Contreras-Porcia, L., Dennett, G., González, A., Vergara, E., Medina, C., Correa, J. A., *et al*., 2011. Identification of copper-induced genes in the marine alga *Ulva compressa* (Chlorophyta). *Marine Biotechnology*, **13** (3): 544-556, DOI: 10.1007/s10126-010-9325-8.

Darko, E., Ambrus, H., Stefanovits-Banyai, E., Fodor, J., Bakos, F., and Barnabas, B., 2004. Aluminium toxicity, Al tolerance and oxidative stress in an Al-sensitive wheat genotype and in Al-tolerant lines developed by *in vitro* microspore selection. *Plant Science*, **166** (3): 583-591, DOI: 10.1016/j.plantsci.2003.10.023.

Dawood, M., Cao, F., Jahangir, M. M., Zhang, G., and Wu, F., 2012. Alleviation of aluminum toxicity by hydrogen sulfide is related to elevated ATPase, and suppressed aluminum uptake and oxidative stress in barley. *Journal of Hazardous Materials*, **s209-210** (1): 121-128, DOI: 10.1016/j.jhazmat.2011.12.076.

Ding, Y., Miao, J. L., Li, G. Y., Wang, Q. F., Kan, G. F., and Wang, G. D., 2005. Effect of Cd on GSH and GSH-related enzymes of *Chlamydomonas* sp. ICE-L existing in Antarctic ice. *Journal of Environmental Sciences*, **17** (4): 667-671, DOI: 10.1007/s11769-005-0024-8.

Dixon, D. P., and Edwards, R., 2010. Roles for stress-inducible lambda glutathione transferases in flavonoid metabolism in plants as identified by ligand fishing. *Journal of Biologycal Chemistry*, **285** (47): 36322-36329, DOI: 10.1074/jbc.M110.164806.

Ducat, D. C., Sachdeva, G., and Baker, S. D., 2011. Rewiring hydrogenase-dependent redox circuits in cyanobacteria. *Proceedings of the National Academy of Sciences of the United States of America*, **108** (10): 3941-3946, DOI: 10.2307/41061040.

Edwards, R., Dixon, D. P., Cummins, I., Brazier-Hicks, M., and Skipsey, M., 2011. New perspectives on the metabolism and detoxification of synthetic compounds in plants. In: *Organic Xenobiotics and Plants*. Schröder, P., and Collins, C. D., eds., Springer, Berlin, 125-148.

Feng, L. X., 2006. Effects of environmental stress on the chlorophy fluorescence of 4 microalgal strains. Master thesis. Ocean University of China (in Chinese with English abstract).

Fernandes, J. C., and Henriques, F. S., 1991. Biochemical, physiological, and structural effects of excess copper in plants. *Botanical Review*, **57** (3): 246-273, DOI: 10.2307/4354171.

Frova, C., 2003. The plant glutathione transferase gene family:

Genomic structure, functions, expression and evolution. *Plant Physiology*, **119** (4): 469-479, DOI: 10.1046/j.1399-3054.2003.00183.x.

Genty, B., Briantais, J. M., and Baker, N. R., 1989. The relationship between the quantum yield of photosynthetic electron transport and quenching of chlorophyll fluorescence. *Biochimica et Biophysica Acta-General Subjects*, **990** (1): 87-92, DOI: 10.1016/S0304-4165(89)80016-9.

Gill, T., Dogra, V., Kumar, S., Ahuja, P. S., and Sreenivasulu, Y., 2011. Protein dynamics during seed germination under copper stress in *Arabidopsis* overexpressing Potentilla superoxide dismutase. *Journal of Plant Research*, **125** (1): 165-172, DOI: 10.1007/s10265-011-0421-2.

Han, X. M., Yang, Z. L., Liu, Y. J., Yang, H. L., and Zeng, Q. Y., 2018. Genome-wide profiling of expression and biochemical functions of the *Medicago* glutathione S-transferase gene family. *Plant Physiology and Biochemistry*, **126** (1): 126-133, DOI: 10.1016/j.plaphy.2018.03.004.

Hauke, J., and Kossowski, T., 2011. Comparison of values of Pearson's and Spearman's correlation coefficients on the same sets of data. *Geographie Physique Quaternaire*, **30** (2): 87-93, DOI: 10.2478/v10117-011-0021-1.

Havaux, M., 1998. Carotenoids as membrane stabilizers in chloroplasts. *Trends in Plant Science*, **3** (4): 147-151, DOI: 10.1016/S1360-1385(98)01200-X.

Herzi, F., Jean, N., Zhao, H. Y., Mounier, S., Mabrouk, H. H., and Hlaili, A. S., 2013. Copper and cadmium effects on growth and extracellular exudation of the marine toxic dinoflagellate *Alexandrium catenella*: 3d-fluorescence spectroscopy approach. *Chemosphere*, **93** (6): 1230-1239, DOI: 10.1016/j.chemosphere 2013.06.084.

Hu, B., Jin, J. P., Guo, A. Y., Zhang, H., Luo, J. C., and Gao, G., 2014. GSDS 2.0: An upgraded gene features visualization server. *Bioinformatics*, **31** (8): 1296-1297, DOI: 10.1093/bioinformatics/btu817.

Hurd, C. L., Harrison, P. J., Bischof, K., and Lobban, C. S., 2014. Physico-chemical factors as environmental stressors in seaweed biology. In: *Seaweed Ecology and Physiology*. Cambridge University Press, London, 294-348.

Jiang, C. D., Gao, H. Y., and Zou, Q., 2003. Changes of donor and accepter side in photosystem II complex induced by iron deficiency in attached-soybean and maize leaves. *Photosynthetica*, **41** (2): 267-271, DOI: 10.1023/B:PHOT.0000011960.95482.91.

Khan, W., Rayirath, U. P., Subramanian, S., Jithesh, M. N., Rayorath, P., Hodges, D. M., *et al*., 2009. Seaweed extracts as biostimulants of plant growth and development. *Journal of Plant Growth Regulation*, **28** (4): 386-399, DOI: 10.1007/s00344-009-9103-x.

Kumar, S., Stecher, G., Li, M., Knyaz, C., and Tamura, K., 2018. MEGA X: Molecular evolutionary genetics analysis across computing platforms. *Molecular Biology and Evolution*, **35** (6): 6, DOI: 10.1093/molbev/msy096.

Lan, T., Yang, Z. L., Yang, X., Liu, Y. J., Wang, X. R., and Zeng, Q. Y., 2009. Extensive functional diversification of the *Populus* glutathione S-transferase supergene family. *Plant Cell*, **21** (12): 3749-3766, DOI: 10.1105/tpc.109.070219.

Li, Y. Q., Horsman, M., Wang, B., Wu, N., and Lan, C. Q., 2008. Effects of nitrogen sources on cell growth and lipid accumulation of green alga *Neochloris oleoabundans*. *Applied Microbiology and Biotechnology*, **81** (4): 629-636, DOI: 10.1007/s00253-008-1681-1.

Liang, Y., Feng, L. X., Yin, C. L., and Cao, C. H., 2007. Current status and prospect of chlorophyll fluorescence technique in the study of responses of microalgae to environmental stress. *Marine Sciences*, **31** (1): 71-76 (in Chinese with English abstract).

Liang, Y., Wang, S., Feng, L. X., and Tian, C. Y., 2008. Effects of heavy metal stress on the growth and chlorophyll fluorescence of *Chaetoceros gracilis*. *Periodical of Ocean University of China*, **38** (1): 59-67 (in Chinese with English abstract).

Lichtenthaler, H. K., and Buschmann, C., 2001. Chlorophylls and carotenoids: Measurements and characterization by UV-Vis spectroscopy. In: *Current Protocols in Food Analytical Chemistry*. Wrolstad, R. E., *et al*., eds., John Wiley and Sons, New York, F4.3.1-F4.3.8, DOI: 10.1002/0471142913.faf0402s01.

Liu, H. J., Tang, Z. X., Han, X. M., Yang, Z. L., Zhang, F. M., Yang, H. L., *et al*., 2015. Divergence in enzymatic activities in the soybean GST supergene family provides new insight into the evolutionary dynamics of whole-genome duplicates. *Molecular Biology and Evolution*, **11**: 2844-2859, DOI: 10.1093/molbev/msv156.

Liu, Y. J., Han, X. M., Ren, L. L., Yang, H. L., and Zeng, Q. Y., 2013. Functional divergence of the glutathione S-transferase supergene family in *Physcomitrella patens* reveals complex patterns of large gene family evolution in land plants. *Journal of Plant Physiology*, **161**: 773-786, DOI: 10.1104/pp.112.205815.

Livak, K. J., and Schmittgen, T. D., 2001. Analysis of relative gene expression data using real-time quantitative PCR and the $2^{-\Delta\Delta CT}$ method. *Methods*, **25** (4): 402-408, DOI: 10.1006/meth.2001.

Maxwell, K., and Johnson, G. N., 2000. Chlorophyll fluorescencea practical guide. *Journal of Experimental Botany*, **51** (345): 659-668, DOI: 10.1093/jexbot/51.345.659.

Min, H. T., and Golden, S. S., 2000. A new circadian class 2 gene, opcA, whose product is important for reductant production at night in *Synechococcus elongatus* PCC 7942. *Journal of Systematic Bacteriology*, **182** (21): 6214-6221, DOI: 10.1128/JB.182.21.6214-6221.2000.

Navarrete, I. A., Kim, D. Y., Wilcox, C., Reed, D. C., and Wilcox, B. H., 2021. Effects of depth-cycling on nutrient uptake and biomass production in the giant kelp *Macrocystis pyrifera*. *Renewable and Sustainable Energy Reviews*, **141**: 110747, DOI: 10.1016/j.rser.2021.110747.

Nianiou-Obeidat, I., Madesis, P., Kissoudis, C., Voulgari, G., Chronopoulou, E., Tsaftaris, A., *et al*., 2017. Plant glutathione transferase-mediated stress tolerance: Functions and biotechnological applications. *Plant Cell Reports*, **36** (6): 791-805, DOI: 10.1007/s00299-017-2139-7.

Okamoto, O. K., Asano, C. S., Aidar, E., and Colepicolo, P., 1996. Effects of cadmium on growth and superoxide dismutase activity of the marine microalga *Tetraselmis gracilis* (Prasinophyceae). *Journal of Applied Phycology*, **32**: 74-79, DOI: 10.1111/j.0022-3646.1996.00074.x.

Perrot, T., Rossi, N., A Ménesguen, and Dumas, F., 2014. Modelling green macroalgal blooms on the coasts of Brittany, France to enhance water quality management. *Journal of Marine Systems*, **132**: 38-53, DOI: 10.1016/j.jmarsys.2013.12.010.

Plekhanov, S. E., and Chemeris, Y. K., 2003. Early toxic effects of zinc, cobalt, and cadmium on photosynthetic activity of the green alga *Chlorella pyenoidosa* chick S-39. *Biological Bulletin*, **30** (5): 506-511, DOI: 10.1023/A:1025806921291.

Rijstenbil, J. W., and Gerringa, L. J. A., 2002. Interactions of algal ligands, metal complexation and availability, and cell responses of the diatom *Ditylum brightwellii* with a gradual increase in copper. *Aquatic Toxicology*, **56** (2): 115-131, DOI: 10. 1016/s0166-445x(01)00188-6.

Rijstenbil, J. W., Derksen, J., Gerringa, L., Poortvliet, T., and Wijnholds, J. A., 1994. Oxidative stress induced by copper: Defense and damage in the marine planktonic diatom *Dictylum brightwellii* grown in continuous cultures with high and low zinc levels. *Marine Biology*, **119**: 583-590, DOI: 10.1007/BF 00354321.

Sandmann, G., and Böger, P., 1980. Copper defieciency and toxicity in *Scenedesmus*. *Zeitschrift für Pflanzenphysiologie*, **98** (1): 53-59, DOI: 10.1016/S0044-328X(80)80219-4.

Sharma, R., Brown, D., Awasthi, S., Yang, Y., Sharma, A., Patrick, B., *et al*., 2004. Transfection with 4-hydroxynonenal-metabolizing glutathione S-transferase isozymes leads to phenotypic transformation and immortalization of adherent cells. *Febs Journal*, **271** (9): 1690-1701, DOI: 10.1111/j.1432-1033.2004.04067.x.

Shukla, P., and Edwards, M. S., 2017. Elevated pCO_2 is less detrimental than increased temperature to early development of the giant kelp, *Macrocystis pyrifera* (Phaeophyceae, Laminariales). *Phycologia*, **56** (6): 638-648, DOI: 10.2216/16-120.1.

Simkovsky, R., Daniels, E. F., Tang, K., Huynh, S. C., Golden, S. S., and Brahamsha, B., 2012. Impairment of O-antigen production confers resistance to grazing in a model amoeba-cyanobacterium predator-prey system. *Proceedings of the National Academy of Sciences of the United States of America*, **109** (41): 16678-16683, DOI: 10.1073/pnas.1214904109.

Smith, P. K., Krohn, R. I., and Hermanson, G. T., 1985. Measurement of protein using bicinchoninic acid. *Analytical Biochemistry*, **163** (1): 76-85, DOI: 10.1016/0003-2697(85)90442-7.

Stauber, J. L., and Florence, T. M., 1989. The effect of culture medium on metal toxicity to the marine diatom *Nitzschia closterium* and the freshwater green alga *Chlorella pyrenoidosa*. *Journal of Applied Water Engineering and Research*, **23** (7): 907-911, DOI: 10.1016/0043-1354(89)90016-X.

Taniguchi, Y., Nishikawa, T., Kondo, T., and Oyama, T., 2012. Overexpression of lalA, a paralog of labA, is capable of affecting both circadian gene expression and cell growth in the cyanobacterium *Synechococcus elongatus* PCC 7942. *Febs Letters*, **586** (6): 753-759, DOI: 10.1016/j.febslet.2012.01.035.

Wagner, U., Edwards, R., Dixon, D. P., and Mauch, F., 2002. Probing the diversity of the *Arabidopsis* glutathione S-transferase gene family. *Plant Molecular Biology*, **49** (5): 515-532, DOI: 10.1023/A:1015557300450.

Wang, Y. T., Fan, X., Gao, G., Beardall, J., and Ye, N. H., 2020. Decreased motility of flagellated microalgae long-term acclimated to CO_2-induced acidified waters. *Nature Climate Change*, **10** (6): 561-567, DOI: 10.1038/s41558-020-0776-2.

Wiencke, C., and Bischof, K., 2012. *Seaweed Biology: Novel Insights into Ecophysiology, Ecology and Utilization*. Springer, Berlin, 507pp.

Xiao, L., Gao, R. F., and Sui, F. G., 2008. Effects of chloride stress on the photosynthesis and chlorophyll content of Chinese cabbage seedlings. *Soil and Fertilizer Sciences in China*, **2** (2): 44-47 (in Chinese with English abstract).

Yang, G. Y., Wang, Y. C., Xia, D., Gao, C. Q., Wang, C., and Yang, C, P., 2014a. Overexpression of a GST gene (ThGSTZ1) from *Tamarix hispida* improves drought and salinity tolerance by enhancing the ability to scavenge reactive oxygen species. *Plant Cell Tissue and Organ Culture*, **117** (1): 99-112, DOI: 10.1007/s11240-014-0424-5.

Yang, Q., Liu, Y. J., and Zeng, Q. Y., 2014b. Biochemical functions of the glutathione transferase supergene family of *Larix kaempferi*. *Plant Physiology and Biochemistry*, **77**: 99-107, DOI: 10.1016/j.plaphy.2014.02.003.

Zar, J., 1999. *Biostatistical Analysis*. Prentice-Hall, Englewood Cliffs, 941pp.

Zhang, C. H., Wu, Z. Y., Ju, T., and Ge, Y., 2013. Purification and identification of glutathione-S-transferase in rice root under cadmium stress. *Rice Science*, **20** (3): 173-178, DOI: 10.1016/s1672-6308(13)60114-6.

Zhang, G. J., Jiang, H., Zheng, L. Q., Chen, J., Qiu, D. L., and Liu, X. H., 2009. Effect of copper stress on photosynthesis of navel orange seedlings. *Chinese Journal of Eco-Agriculture*, **17** (1): 130-134, DOI: 10.3724/SP.J.1011.2009.00130 (in Chinese with English abstrwact).

Zhang, X. W., Zhang, J., Wang, Y. T., Xu, D., and Ye, N. H., 2021. The oxylipin messenger 1, ctenl induced rapid responses in kelp *Macrocystis pyrifera*. *Physiologia Plantarum*, **172**: 1641-1652, DOI: 10.1111/ppl.13358.

Zhang, Y. F., Gu, Z. P., Ren, Y. D., Wang, L., Zhang, J., Liang, C. W., *et al*., 2021. Integrating transcriptomics and metabolomics to characterize metabolic regulation to elevated CO_2 in *Chlamydomonas Reinhardtii*. *Marine Biotechnology (NY)*, **23** (2): 255-275, DOI: 10.1007/s10126-021-10021-y.

(Edited by Qiu Yantao)